

28.1 A Handheld 50pM-Sensitivity Micro-NMR CMOS Platform with B-Field Stabilization for Multi-Type Biological/Chemical Assays

Ka-Meng Lei¹, Hadi Heidari^{2,3}, Pui-In Mak¹, Man-Kay Law¹, Franco Maloberti², Rui P. Martins^{1,4}

¹University of Macau, Macau, China,

²University of Pavia, Pavia, Italy,

³University of Glasgow, Glasgow, United Kingdom,

⁴Instituto Superior Tecnico, Lisbon, Portugal

Point-of-use (PoU) biological/chemical assays are aimed to transform bulky laboratory instruments into easy-to-use lab-on-a-chip platforms, bringing down the cost, size, and sample-use by orders of magnitude [1,2]. Micro-Nuclear Magnetic Resonance (NMR) is a trail-blazing tool for *target* pinpointing, by utilizing functionalized magnetic nanoparticles (MNPs) as the *probe* [3]. Screening by micro-NMR is repeatable, versatile and low-cost as it is label- and washing-free for the samples, and immobilization-free for the electrodes. Herein, a high-sensitivity micro-NMR CMOS platform with magnetic (B)-field stabilization and thermal management is reported (Fig. 28.1.1). This handheld tool unifies multi-type assays (target detection, protein state analysis, and solvent-polymer dynamics), and is suitable for healthcare, food industry, and colloidal applications.

Micro-NMR relaxometry detects the spin-spin relaxation time (T_2) by extracting the echoes envelopes from the response of the non-zero spin nuclei (i.e., ^1H). The nuclei, under magnetization with a static magnetic field (B_0), absorb orthogonal RF exciting magnetic field (B_1) at the Larmor frequency, $f_L = \gamma B_0$ (γ : gyromagnetic ratio), and precess about the direction of magnetization at f_L even after the cessation of the excitation. In an existing micro-NMR system [3], frequency deviation of the local oscillator (LO) from f_L induces improper frequency excitation, paralyzing the operation. Confounded by the thermal instability of the portable magnet ($B_0=0.46\text{T}$, T.C.= -1200ppm/K), LO tracking is essential to safeguard the system against environmental changes.

Our micro-NMR platform (Fig. 28.1.2) is tailored with B_0 -field stabilization and thermal management to enhance the robustness and simplify the hardware. The dynamic B_1 -field transduction is based on a spiral coil driven by a transmitter (TX)/receiver (RX) together with a matching capacitor C_m , to excite/obtain the magnetic signal to/from the droplet samples (2.5 μL) normal to the chip surface. The TX is based on a tapped inverter-chain power amplifier (PA), measured 31.6% power efficiency, to deliver programmable pulse sequences pertaining to the LO. The RX features a multi-stage low-noise amplifier (LNA) for high RX sensitivity (down to 1nV/ $\sqrt{\text{Hz}}$ input-referred-noise), and a dynamic-bandwidth lowpass filter for fast recovery from saturation after excitation pulses. The B_0 -field sensor and calibrator manage the lateral B_0 -field together with a current driver, which injects a calibration current to the magnet (75mT/A) stabilizing the bulk magnetization on the nuclei. The spiral coil also serves as a heater allowing thermal profiling of the samples. The thermal-induced error on the B_0 -field sensor and calibrator, and the hotness of the samples, are monitored by a BJT temperature sensor.

To sense the lateral B_0 -field normal to the chip surface, a *current-mode* 4-folded vertical hall sensor (VHS) arranged in a Wheatstone bridge is employed (Fig. 28.1.3). Each VHS element is composed by an n-well as the substrate and three n-diffusions as contacts [4]. P-diffusions are embedded between the n-diffusions to avert current flowing at the surface, soothing the $1/f$ noise. To achieve sub-nA sensitivity, the VHS readout circuit (Fig. 28.1.3) is based on a low-noise TIA. Current-spinning and chopper are applied reducing the $1/f$ noise corner by $>5,000\times$. Switches $S_{7,8}$ control the flows of the current and reset the capacitors C_F . Small switches (280 Ω each) can exacerbate the impedance of the TIA, ($R_{in,TIA}=210\Omega$) if there is current passing through the switches connected between the core OTA of the TIA and VHS (i.e., $S_{5,6}$). To address this, $S_{7,8}$ are managed to guide the current passing through the negative feedback path, nullifying the impact of resistances of $S_{5,6}$ on the TIA. Thanks to this switching scheme, $R_{in,TIA}$ is suppressed by 84%, absorbing $\sim 21\%$ more current into the TIA than the general approach [5].

Attributed to the prodigious nominal B_0 -field, a typical TIA can be saturated and fail to sense the tiny B_0 -field variation (3.75mT). To solve it, a nominal B_0 -field compensator made by a passive switched-capacitor network (Fig. 28.1.3) nullifies the nominal B_0 -field entering into the TIA.

Before the micro-NMR assay, the VHS reads B_0 and responds to the current driver (Fig. 28.1.4). B_0 may shift away from its nominal value due to the environmental changes (e.g., temperature and sample-to-magnet position). Thus, untracked f_L can be easily off-center from the LO frequency f_{osc} (BW=16.7kHz). Here, by modulating the magnet according to an updated B_0 (sensitivity: 4.12V/T), f_L is reset to f_{osc} . Also, with signal-averaging performed in the frequency domain to suppress the background noise, the calibration improves the B_0 -field stability by $13\times$ (from 2 to 0.15mT) at 0.46T ($f_L=19.6\text{MHz}$). Under the synergy of micro-NMR and VHS, the stabilized f_L inspires the use of a simple crystal oscillator as the LO that measures low phase noise (-116dBc/Hz at 1kHz offset) at very low power (79 μW).

Human Immunoglobulin G (IgG), which protects the body from infections, can be quantified by utilizing Protein A coated water-soluble MNPs (i.e., Fe_3O_4) based on their T_2 . T_2 of the sample is shortened commensurate with the amount of IgG upon nanoparticles agglomeration, enabling quantification of IgG down to 5nM (Fig. 28.1.5). The specificity of micro-NMR assay is evinced with the addition of Chicken Immunoglobulin Y (IgY), which does not conjugate with Protein A. The negligible change of T_2 ($<2\%$) validates the selectivity of the assay. The versatility of the platform is manifested with DNA detection apt for life-threatening bacteria screening. With a pair of probe-decorated MNPs, the platform quantifies the synthesized DNA derived from *Enterococcus faecalis*, with a detection limit down to 50pM in 2.5 μL samples (125amol). By varying the MNP concentration, the detection range is impelled to 125nM. The response to single-nucleotide polymorphism is indistinguishable to T_2 baseline ($<4\%$), substantiating that single-base mismatch DNA can be differentiated.

Probing the molecular structure can digest the protein state for food quality inspection. Protein β -lactoglobulin (β -LG) denatures and aggregates irreversibly after heating to $>60^\circ\text{C}$ [6]. This state transformation can be embodied by measuring T_2 of the samples attributed to the dissimilar interaction between the water molecules and protein at different states and sizes (Fig. 28.1.6). For the colloidal industry, Poly(N-isopropylacrylamide) (PNIPAM) is widely used as advanced sensor and drug delivery carrier [7]. It is a colloidal polymer that exhibits a temperature-induced reversible volume phase transition in water, affects the local environment on solvent confinement and thus T_2 of the solvent. By duty-cycling the heater (coil), PNIPAM undergoes a volume phase transition above 33°C , resulting in T_2 decrement of the solvent.

Benchmarking with the recent PoU tools (Fig. 28.1.7), this work supports multi-type assays in one unified platform, while achieving high sensitivity and selectivity for DNA, as well as other proteins targeting capability in tiny sample with functionalized MNPs. The platform consumes $120\times$ less samples, and is $96\times$ lighter, $175\times$ smaller, and $16\times$ cheaper than a commercial product (Bruker mq-20 [8]).

Acknowledgements:

The authors thank Macao FDCT (SKL fund & 047/2014/A1) for financial support.

References:

- [1] M. Bakhshiani et al., "A Microfluidic-CMOS Platform with 3D Capacitive Sensor and Fully Integrated Transceiver IC for Palmtop Dielectric Spectroscopy," *ISSCC Dig. Tech. Papers*, pp. 386-387, Feb. 2015.
- [2] P.-H. Kuo et al., "A Smart CMOS Assay SoC for Rapid Blood Screening Test of Risk Prediction," *ISSCC Dig. Tech. Papers*, pp. 390-391, Feb. 2015.
- [3] N. Sun et al., "Palm NMR and One-Chip NMR," *ISSCC Dig. Tech. Papers*, pp. 488-489, Feb. 2010.
- [4] G.-M. Sung et al., "2-D Differential Folded Vertical Hall Device Fabricated on a P-Type Substrate Using CMOS Technology" *IEEE Sensors J.*, vol. 13, pp. 2253-2262, June 2013.
- [5] H. Heidari et al., "A CMOS Current-Mode Magnetic Hall Sensor with Integrated Front-end," *IEEE Trans. Circuits Syst. I*, vol. 62, no. 5, pp. 1270-1278, May 2015.
- [6] L. Indrawati et al., "Low-Field NMR: A Tool for Studying Protein Aggregation," *J. Sci. Food Agric.*, vol. 87, pp. 2207-2216, Sept. 2007.
- [7] B. S.-Martin et al., "Structure and Polymer Dynamics within PNIPAM-Based Microgel Particles," *Adv. Colloid Interface Sci.*, vol. 205, pp. 113-123, Mar. 2014.
- [8] Bruker Minispec Contrast Agent Analyzer, [Online]. Available: <https://www.bruker.com/products/mr/td-nmr/minispec-mq-series/mq-contrast-agent-analyzer/overview.html>

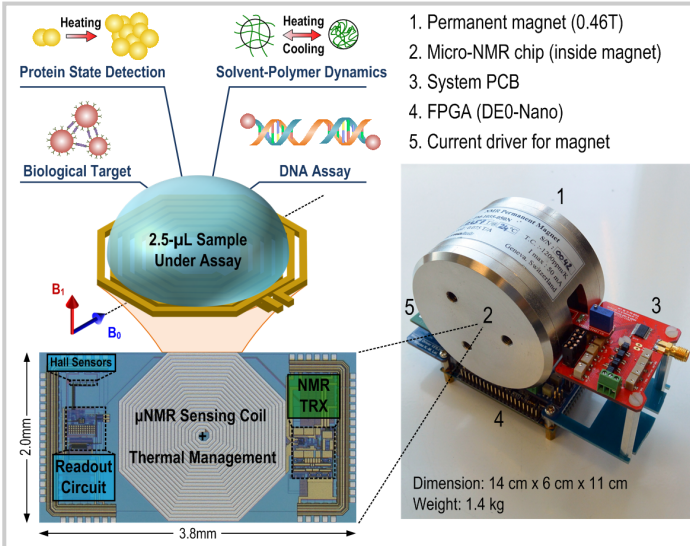


Figure 28.1.1: A micro-NMR CMOS platform with B-field stabilization: (left) chip photo and (right) platform assembly.

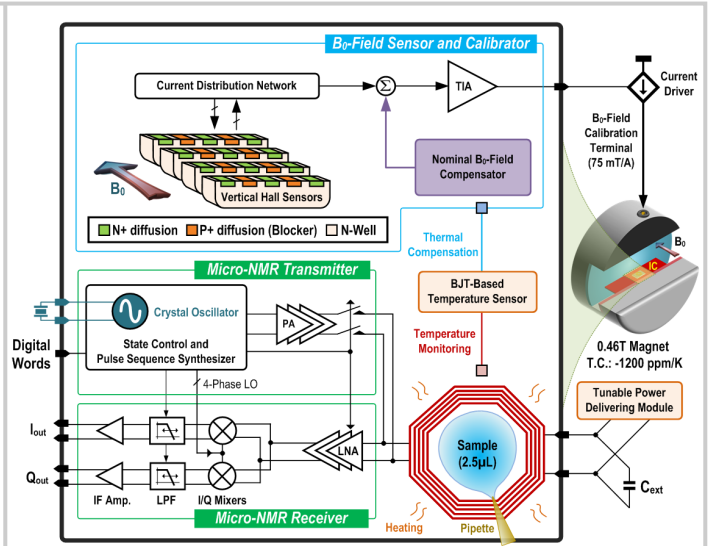


Figure 28.1.2: System block diagram.

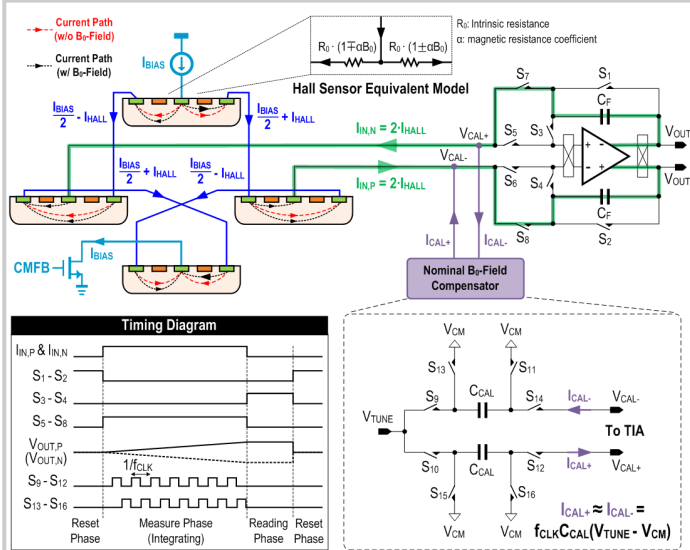


Figure 28.1.3: Current-mode 4-folded VHS to sense the lateral B_0 -field.

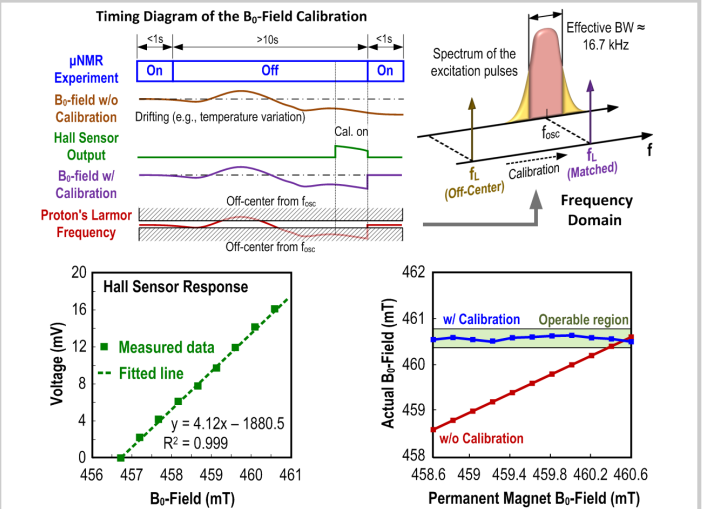


Figure 28.1.4: (Top) Timing diagram of the B_0 -field calibration and its frequency domain illustration. (Bottom) Measured Hall sensor response and B_0 -field with and without calibration.

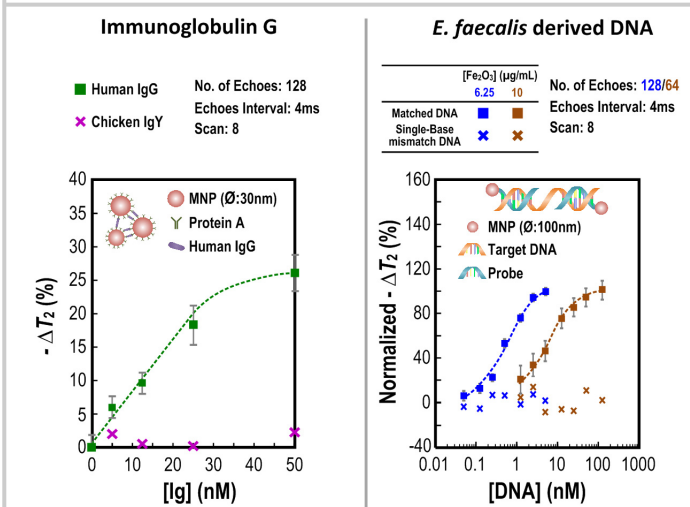


Figure 28.1.5: Examples of target detection: (left) from Human IgG as target, and Chicken IgY as control; (right) from *E. faecalis* derived DNA and single-base mismatch DNA.

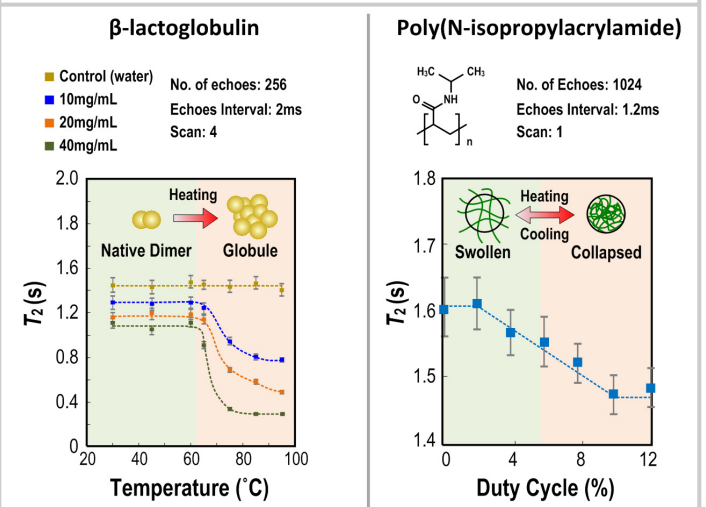


Figure 28.1.6: Examples of state analysis reflected by T_2 : (left) thermal profiling of protein (β -LG) state; (right) polymer (PNIPAM) dynamics during heating and cooling.

	This Work	P.-H. Kuo <i>et al.</i> , ISSCC'15	K.-H. Lee <i>et al.</i> , ISSCC'12	N. Sun <i>et al.</i> , ISSCC'10	B. Jang <i>et al.</i> , ISSCC'09	
Application	Specificity	1. Target detection 2. Solvent-Polymer dynamics 3. Protein state analysis	Target detection	Target detection	Target detection	Target detection
	Target Labeling	Label-free	Label-free	Label-free	Label-free	Cy5-label
	Demo Target	68 base <i>E. faecalis</i> derived DNA	NT-ProBNP & TNF-alpha	21 base H5N1 virus	hCG cancer marker	18 base DNA
	Detection Limit	50 pM (DNA)	--	100 pM (DNA)	5000 pM (Cancer marker)	125 pM (DNA)
	Sample Handling Limit	2.5 μ L	--	--	5.0 μ L	--
Hardware	Physics	NMR relaxometry + Thermal management	Magnetic- sensing	Capacitance- sensing	NMR relaxometry	Fluorescent- sensing
	Post-Fabrication Necessity	No (immobilization free)	Probe (antibody) immobilization	Probe (DNA) immobilization on Au electrodes	No (immobilization free)	Fiber-optical faceplate
	External Part	Portable magnet	No	No	Portable magnet	Light source
	LO Generation	Crystal oscillator + B_z -field calibration	--	--	Off-chip	--
	Robustness to environments	Robust to temperature & sample position variations	Robust to temperature variation	Vulnerable to bias current variation	Vulnerable to B_z -field variation	Vulnerable to background noise
	CMOS Tech.	0.18 μ m	0.35 μ m	0.35 μ m	0.18 μ m	0.35 μ m
	Chip Area	7.6 mm ²	8.9 mm ²	20.0 mm ²	11.3 mm ²	9.0 mm ²

Figure 28.1.7: Benchmark with other CMOS-based PoU systems.